Protein Engineering, Design & Selection vol. 23 no. 4 pp. 229–241, 2010
Published online November 27, 2009 doi:10.1093/protein/gzp074

Knowledge-based design of reagentless fluorescent biosensors from a designed ankyrin repeat protein

Elodie Brient-Litzler[1], Andreas Plückthun[2] and Hugues Bedouelle[1,3]

[1]Unit of Molecular Prevention and Therapy of Human Diseases (CNRS URA3012), Institut Pasteur, 25 rue Docteur Roux, 75724 Paris Cedex 15, France and [2]Biochemisches Institut, Universität Zürich, Winterthurerstr. 190, 8057 Zürich, Switzerland

[3]To whom correspondence should be addressed.
E-mail: hugues.bedouelle@pasteur.fr

Received October 21, 2009; revised October 21, 2009; accepted October 27, 2009

Edited by Andrew Bradbury

Designed ankyrin repeat proteins (DARPins) can be selected from combinatorial libraries to bind any target antigen. They show high levels of recombinant expression, solubility and stability, and contain no cysteine residue. The possibility of obtaining, from any DARPin and at high yields, fluorescent conjugates which respond to the binding of the antigen by a variation of fluorescence, would have numerous applications in micro- and nano-analytical sciences. This possibility was explored with Off7, a DARPin directed against the maltose binding protein (MalE) from *Escherichia coli*, with known crystal structure of the complex. Eight residues of Off7, whose solvent accessible surface area varies on association with the antigen but which are not in direct contact with the antigen, were individually mutated into cysteine and then chemically coupled with a fluorophore. The conjugates were ranked according to their relative sensitivities. All of them showed an increase in their fluorescence intensity on antigen binding by >1.7-fold. The best conjugate retained the same affinity as the parental DARPin. Its signal increased linearly and specifically with the concentration of antigen, up to 15-fold in buffer and 3-fold in serum when fully saturated, the difference being mainly due to the absorption of light by serum. Its lower limit of detection was equal to 0.3 nM with a standard spectrofluorometer. Titrations with potassium iodide indicated that the fluorescence variation was due to a shielding of the fluorescent group from the solvent by the antigen. These results suggest rules for the design of reagentless fluorescent biosensors from any DARPin.

Keywords: ankyrin repeat protein (DARPin)/antibody/biosensor/fluorescence/protein design

Introduction

The detection and quantitation of biomolecules in crude mixtures is a general problem in bioanalytical sciences and diagnostics. Although the problem of their specific recognition has been solved by using either antibodies or artificial binding proteins, the problem of sensing and recording the binding event needs to be addressed separately. In most analytical systems, this problem has been solved by immobilizing one of the molecular partners or labeling the biomolecules of the mixture under analysis, which is time-consuming and involves complex liquid handling. In a molecular biosensor, a recognition module and a transduction module, which transforms the recognition event into a measurable signal, are integrated into a compact device with molecular dimensions (Lowe, 1984). Such a biosensor ideally functions without additional reagent, provides quantitative analytical information and follows the concentration of its molecular target, called analyte, continuously (Thevenot *et al*., 2001). Here, we describe the development of molecular biosensors that can be obtained through a straightforward design, are robust, give immediate responses and can work in homogeneous solutions.

Fluorescence allows one to detect molecular interactions with great sensitivity. The transduction is based on a variation of the fluorescence properties of the biosensor when it interacts with its analyte (Altschuh *et al*., 2006). The fluorescence of a protein biosensor can be intrinsic, e.g. provided by its component residues of tyrosine and tryptophan, or extrinsic, e.g. provided by the coupling of fluorescent groups that absorb and emit light outside of the protein spectral region. While intrinsic protein fluorescence can be used to study molecular interactions in purified experimental systems, extrinsic fluorescence is preferable to monitor specific interactions in complex media (Foote and Winter, 1992). The coupling of several fluorophores to a unique molecule of biosensor can be used to measure changes in distances but is usually difficult to implement and needs to be adjusted for every new system (Smith *et al*., 2005). For these reasons, we gave preference to reagentless fluorescent (RF) biosensors that derive from protein receptors and whose fluorescence is provided by the coupling of a single extrinsic fluorophore.

The changes of fluorescence that occur upon recognition between an RF biosensor and its analyte result from changes in the environment of the fluorescent group between the free and bound forms of the biosensor. The binding of the analyte can occur in the neighborhood of the fluorescent group and directly modify its environment. Alternatively, the binding of the analyte can induce a conformational change of the biosensor and thus alter the interaction between the fluorescent group and the receptor indirectly. We and others used the first mechanism to create RF biosensors from antibodies, first when the three-dimensional structure of the complex with their antigen is known and then in the absence of such a knowledge (Renard *et al*., 2002, 2003; Jespers *et al*., 2004; Renard and Bedouelle, 2004). Other groups used the second mechanism to create biosensors from periplasmic binding proteins (de Lorimier *et al*., 2002). In both cases, a cysteine residue is introduced by site-directed mutagenesis in a pre-determined position of the receptor and

a fluorophore is chemically coupled to this unique residue of cysteine.

Antibodies are perfectly suited to provide the recognition module of biosensors since they can be directed against any antigen. However, they have several intrinsic limitations. The single-chain variable fragments, or scFv, which have served as starting molecules for the construction of biosensors, often have insufficient conformational stabilities and *in vitro* half-lives for use in prolonged or harsh conditions. They contain two disulfide bonds, one in each variable domain. Therefore, they must be exported into the oxidizing medium of the bacterial periplasm to obtain the formation of their disulfide bonds and their folding in a functional state. This periplasmic expression limits their yield of production. The mutant cysteine, to which the fluorophore is chemically coupled, often needs to be reactivated by a mild reduction before coupling. This reduction partially attacks the disulfide bonds of the fragment and decreases the production yield of the fluorescent conjugate.

The problems of expression and stability that are encountered with most recombinant antibodies slow down their exploitation in various domains of application. These problems led several groups to develop alternative families of antigen binding proteins, by engineering proteins that have a stable polypeptide scaffold, are devoid of cysteine residue and disulfide bond and are well expressed in *Escherichia coli*. These new families of antigen binding proteins can replace antibodies in many of their applications (Mathonet and Fastrez, 2004; Binz *et al*., 2005). The designed ankyrin repeat proteins (DARPins) illustrate the potential of these artificial families of antigen binding proteins. The repeated ankyrin modules are present in thousands of proteins from all phyla and involved in specific recognition between proteins (Mosavi *et al*., 2004; Li *et al*., 2006). Consensus sequences of these modules have been established and the corresponding consensus proteins shown to possess remarkable biophysical properties. Their stability ($t_{1/2} > 65^{\circ}C$), solubility (several mM) and production yield in the cytoplasm of *E.coli* (up to 200 mg/l of culture in flask) are more favorable than those of antibody fragments (Mosavi *et al*., 2002; Binz *et al*., 2003; Kohl *et al*., 2003). Combinatorial libraries of DARPins have been generated by randomization of residues that potentially belong to the paratope (antigen binding site), and assemblage of a few ankyrin modules between defined N- and C-terminal modules (Binz *et al*., 2003). These libraries were used to select DARPins that bound specific protein antigens, by ribosome or phage display (Zahnd *et al*., 2007; Steiner *et al*., 2008). DARPins with high affinities and specificities have been obtained against a wide variety of protein antigens and their development as therapeutic molecules initiated (Stumpp *et al*., 2008).

We show here that the methods that we have developed to design and construct RF biosensors from antibodies can be extended to new families of antigen binding proteins and that it is possible to directly profit from their more favorable properties. We describe rules for the design of RF biosensors from DARPins when the three-dimensional structure of the complex with their target antigen is known, and the validation of these rules with Off7, a DARPin which is directed against the maltose binding protein (MalE) from *E.coli* (Binz *et al*., 2004).

Materials and methods

Analysis of the structural data

The crystal structure of the complex between Off7 and MalE (PDB 1SVX) was analyzed with the program What If (Vriend, 1990). The solvent accessible surface areas (ASA) were calculated with the ACCESS routine and a radius of the solvent sphere equal to 1.4 Å. The contact residues between Off7 and MalE were identified with the ANACON routine, using extended van der Waals radii as described (Rondard and Bedouelle, 1998). Water molecules bridging Off7 and MalE were identified with the subroutine NALWAT. The three-dimensional structures of the cysteine mutants of Off7 were modeled with the mutation prediction program of the What If web interface (http://swift.cmbi.kun.nl/whatif/).

Materials

The *E.coli* strains XL1-Blue (Bullock *et al*., 1987) and AVB99 (Smith *et al*., 1998), and plasmids pQEMBP, pAT224 and pQEOff7 (Binz *et al*., 2004) have been described. pQEMBP codes for the maltose binding protein MalE from *E.coli*; pAT224, for a hybrid bt-MalE between an N-terminal AviTag that can be enzymatically biotinylated, and MalE; pQEOff7, for the DARPin Off7, directed against MalE. All the recombinant proteins carry a hexahistidine tag. Buffer H was 500 mM NaCl, 50 mM Tris–HCl (pH 7.5); buffer M1, 150 mM NaCl, 50 mM Tris–HCl (pH 7.5); buffer L1, 50 mM NaCl, 20 mM Tris–HCl (pH 7.5); buffer M2, 0.005% (v/v) P20 surfactant (Biacore) in buffer M1; buffer L2, 0.005% (v/v) P20 surfactant in buffer L1; buffer M3, 5 mM dithiothreitol (DTT) in buffer M2. Phosphate buffered saline (PBS), calf serum, hen egg white lysozyme, DTT, Tween 20 and tris(2-carboxyethyl)phosphine (TCEP) were purchased from Sigma, bovine serum albumin (BSA) from Roche, *N*-((2-(iodoacetoxy)ethyl)-*N*-methyl)amino-7-nitrobenz-2-oxa-1,3-diazole (IANBD ester) from Invitrogen. A stock solution of the IANBD ester was made at a concentration of 10 mg/ml in dimethylformamide. Ampicillin was used at a concentration of 100 μg/ml and chloramphenicol at 10 μg/ml.

Mutagenesis and gene synthesis

Changes of residues were introduced by mutagenesis of plasmid pQEOff7 with the Quickchange II site-directed mutagenesis kit (Stratagene). Because the DARPins are constituted of repeated modules of polypeptide and encoded by repeated segments of DNA, the mutagenic primers were designed such that their 3′-nucleotide or the preceding nucleotide was specific for the targeted segment and their elongation by DNA-polymerase could not occur on another repeated segment. Mutation K122C could not be obtained in this way. We therefore used the degeneration of the genetic code to design a mutant allele of the *off7* gene that was devoid of extensive repetitions. The mutant allele, *off7-1*, was synthesized by Genecust (Evry, France) and used to construct mutations K68C and K122C.

Protein production, purification and characterization

The MalE protein was produced in the cytoplasm of the recombinant strain XL1-Blue(pQEMBP), bt-MalE in strain AVB99(pAT224) and Off7 and its mutant derivatives in XL1-Blue(pQEOff7) and its mutant derivatives, as described

(Binz *et al*., 2003; Binz *et al*., 2004). They were purified through their hexahistidine tag by affinity chromatography on a column of fast-flow Ni-NTA resin (Qiagen). The purification fractions were analyzed by SDS–PAGE, with the NuPAGE Novex system, MES buffer and See blue prestained standards (all from Invitrogen). Equal amounts of protein were loaded on the gels after heat denaturation either in the presence or in the absence of 2.5% (v/v, 0.4 M) 2-mercaptoethanol. The gels were stained with Coomassie blue and the protein bands were quantitated with the Un-scan-it software (Silk Scientific). The fractions that were pure after SDS–PAGE under reducing conditions (>98% homogeneous) were pooled and kept at −80°C. The protein concentrations were measured by absorbance spectrometry, with coefficients of molar extinction, $\varepsilon_{280}(\text{MalE}) = 66\,350\ \text{M}^{-1}\,\text{cm}^{-1}$, $\varepsilon_{280}(\text{bt-MalE}) = 71\,850\ \text{M}^{-1}\,\text{cm}^{-1}$ and $\varepsilon_{280}(\text{Off7}) = 16\,960\ \text{M}^{-1}\,\text{cm}^{-1}$, calculated as described (Pace *et al*., 1995). Aliquots of the wild-type Off7(wt) and its mutant derivative Off7(N45C) were analyzed by mass spectrometry after extensive dialysis against 65 mM ammonium bicarbonate and lyophilization, as described (Renard *et al*., 2002). All the binding experiments were performed at 25°C.

Indirect ELISA

ELISA experiments were performed in buffer M1 and microtiter plates as described (Harlow and Lane, 1988), except that the wells of the plates were washed three times with 0.05% (v/v) Tween 20 in buffer M1 and three times with buffer M1 alone between each step. The wells were coated with 0.5 μg ml^{-1} Off7 and blocked with 3% BSA (w/v). The immobilized DARPin was incubated with varying concentrations of bt-MalE and potassium iodide (KI) in 1% BSA for 1 h at 25°C. bt-MalE was omitted in the blank wells. The captured molecules of bt-MalE were detected with a conjugate between streptavidin and alkaline phosphatase, and *p*-nitrophenyl phosphate as a substrate (all from Sigma-Aldrich). The absorbance at 405 nm was measured and corrected by subtraction of the blank.

Fluorophore coupling

The cysteine mutants of Off7 were reduced with 5 mM DTT for 30 min at 30°C with gentle shaking and then the buffer was exchanged to PBS by size exclusion chromatography with a PD10 column (GE Healthcare). The thiol-reactive fluorophore IANBD ester was added in >5:1 molar excess over the DARPin and the coupling reaction was carried out for 2 h at 30°C with gentle shaking. The denatured proteins were removed by centrifugation for 30 min at 10 000*g*, 4°C. The conjugate was separated from the unreacted fluorophore by chromatography on an Ni-NTA column and elution with 100 mM imidazole in buffer H. The coupling yield y_c, i.e. the average number of fluorophore molecule coupled to each DARPin molecule, was calculated as described below, with $\varepsilon_{280}(\text{ANBD}) = 2100\ \text{M}^{-1}\,\text{cm}^{-1}$, $\varepsilon_{500}(\text{ANBD}) = 31\,800\ \text{M}^{-1}\,\text{cm}^{-1}$, both measured with conjugates between IANBD and 2-mercaptoethanol (Renard *et al*., 2002).

Let P be a protein; B, a monoconjugate between P and IANBD; Φ, the conjugated form of IANBD; A_{280} and A_{500}, the absorbances of the mixture of P and B that result from the coupling reaction and elimination of the unconjugated fluorophore. By definition,

$$y_c = \frac{[\text{B}]}{[\text{B}] + [\text{P}]} \tag{1}$$

where [B] and [P] are concentrations. Because (i) absorbances are bilinear functions of molar absorbances and concentrations, (ii) the molar absorbances of different chemical groups in a protein molecule are generally additive (Pace *et al*., 1995) and (iii) proteins generally do not absorb at 500 nm, one can write:

$$A_{280} = \varepsilon_{280}(\text{P})[\text{P}] + \varepsilon_{280}(\text{P})[\text{B}] + \varepsilon_{280}(\Phi)[\text{B}] \tag{2}$$

$$A_{500} = \varepsilon_{500}(\Phi)[\text{B}] \tag{3}$$

where ε is a molar absorbance. Equations (2) and (3) can be solved for [B] and [P]. Combining with Equation 1, one obtains for the reciprocal of the coupling yield:

$$y_c^{-1} = \frac{A_{280}}{\varepsilon_{280}(\text{P})}\left(\frac{A_{500}}{\varepsilon_{500}(\Phi)}\right)^{-1} - \frac{\varepsilon_{280}(\Phi)}{\varepsilon_{280}(\text{P})} \tag{4}$$

Thus, the coupling yield can be calculated from measuring A_{500} and A_{280}. Interestingly, the second term in y_c^{-1} is constant and comes from the contribution of Φ to A_{280}.

Fluorescence measurements and antigen binding

We treated the binding and fluorescence experiments at equilibrium as if the preparations of conjugates were homogeneous, i.e. as if $y_c = 1$. The binding reactions were conducted by incubating 0.3 μM of conjugate with variable concentrations of the MalE antigen in a volume of 1 ml, for 1 h in the dark with gentle shaking. The reactions were carried out in buffer L1, buffer M1 or in a mixture v:(1 − v) of calf serum and buffer M1 as indicated in the Results section. The conjugate (or biosensor) B and antigen A form a 1:1 complex B:A according to the reaction:

$$\text{B} + \text{A} \leftrightarrow \text{B:A} \tag{5}$$

At equilibrium, the concentration [B:A] of the complex is given by the equation:

$$[\text{B:A}] = 0.5\{[\text{B}]_0 + [\text{A}]_0 + K_d - (([\text{B}]_0 + [\text{A}]_0 + K_d)^2 - 4[\text{B}]_0[\text{A}]_0)^{1/2}\} \tag{6}$$

where K_d is the dissociation constant, and $[\text{A}]_0$ and $[\text{B}]_0$ are the total concentrations of A and B, respectively (Renard *et al*., 2003).

The fluorescence of the IANBD conjugates was excited at 485 nm (5 nm slit width) and its intensity measured at 535 nm (20 nm slit width) with an LS-5B spectrofluorometer (Perkin-Elmer). The signal of MalE alone was measured in an independent experiment and subtracted from the global signal of the binding mixture to give the specific fluorescence intensity F of each conjugate. The intensity F at a given value of $[\text{A}]_0$ satisfies the following equation:

$$\frac{F - F_0}{F_0} = \frac{\Delta F}{F_0} = \frac{\Delta F_\infty}{F_0}\frac{[\text{B:A}]}{[\text{B}]_0} \tag{7}$$

where F_0 and F_∞ are the values of F at zero and saturating concentrations of A (Renard *et al*., 2003). The values of $\Delta F_\infty/F_0$, $[B]_0$ and K_d could be determined by fitting Equation (7), in which [B:A] is given by Equation (6), to the experimental values of $\Delta F/F_0$, measured in a titration experiment. The fittings were performed with the Kaleidagraph software (Synergy Software).

The sensitivity s and relative sensitivity s_r of a conjugate can be defined by the following equations for the low values of $[A]_0$, i.e. in the initial part of the titration curve:

$$\Delta F = s[A]_0 \tag{8}$$

$$\frac{\Delta F}{F_0} = \frac{s_r[A]_0}{[B]_0} \tag{9}$$

s and s_r can be expressed as functions of characteristic parameters of the conjugate:

$$s_r = \frac{\Delta F_\infty}{F_0}\frac{[B]_0}{K_d + [B]_0} \tag{10}$$

$$s = f_b s_r \tag{11}$$

where $f_b = F_0/[B]_0$ is the molar fluorescence of the free conjugate (Renard and Bedouelle, 2004). Equation (10) implies that s_r is maximal when the biosensor B is present at a concentration $[B]_0 >> K_d$, as every newly titrated molecule A then forms a complex. Equation (8) implies that the lower limit of detection $\delta[A]_0$ of the conjugate is linked to the lower limit of measurement of the spectrofluorometer δF by the following equation:

$$\delta[A]_0 = s^{-1}\delta F = s_r^{-1}[B]_0\frac{\delta F}{F_0} \tag{12}$$

Quenching by potassium iodide

The experiments of fluorescence quenching by KI were performed at 25°C in buffer M1, essentially as described above. The Stern–Volmer Equation (13) was fitted to the experimental data, where F and F^0 are the intensities of fluorescence for the Off7 conjugate in the presence or absence of quencher, respectively. The Stern–Volmer constant K_{SV} was used as a fitting parameter.

$$\frac{F^0}{F} = 1 + K_{SV}[KI] \tag{13}$$

Affinity in solution as determined by competition Biacore

The binding reactions (100 µl) were conducted by incubating 50 nM of Off7 with variable concentrations of MalE in buffer M2 or L2 for 1 h. It results from the laws of mass action and conservation that:

$$[P] = 0.5\{[P]_0 - [A]_0 - K_d + (([P]_0 - [A]_0 - K_d)^2 + 4K_d[P]_0)^{1/2}\} \tag{14}$$

where $[A]_0$ is the total concentration of MalE in the reaction mixture; $[P]_0$ the total concentration of Off7; and [P] the concentration of free Off7 (Lisova *et al*., 2007). The concentration of free Off7 was measured by Biacore, essentially as described (Nieba *et al*., 1996). High densities of bt-MalE (>2000 RU) were immobilized on the surface of a streptavidin SA sensorchip (Biacore). Each reaction mixture was injected in the sensor chip at a flow rate of 25 µl min^{-1}. The chip surface was regenerated by injecting 10 µl of a glycine–HCl solution at pH 3.0 (Biacore) between each run. The experimental data were cleaned up with the Scrubber program (Biologic Software) and analyzed with the Bia-evaluation 2.2.4 program (Biacore) to determine the initial slope r of the association curves, which satisfies the equation (Nieba *et al*., 1996):

$$r = k_{on}R_{max}[P] \tag{15}$$

where k_{on} is the rate constant of association between the free molecules of Off7 and the immobilized molecules of bt-MalE, and R_{max} the resonance signal which is obtained with a saturating concentration of Off7. We checked that R_{max} was not altered by the regeneration of the chip surface and remained constant. Therefore:

$$r = \frac{r_0[P]}{[P]_0} \tag{16}$$

where r_0 is the value of r observed for $[A]_0 = 0$ and therefore $[P] = [P]_0$. The values of K_d and r_0 were determined by fitting Equation (16), in which [P] is given by Equation (14), to the experimental values of r.

Kinetic measurements by Biacore

The kinetics were measured at a flow rate of 25 µl min^{-1} with SA sensor chips. A first cell of the sensor chip was used as a reference, i.e. no ligand was immobilized on the corresponding surface. A second cell was loaded with 500–1000 RU of bt-MalE. Solutions of the Off7 derivatives at eight different concentrations (0.15–400 nM) were injected during 8 min to monitor association and then buffer alone during the same time for dissociation. The chip surface was regenerated between the runs by injecting 5–10 mM NaOH during 1 min. The signal of the buffer alone was subtracted from the raw signals to obtain the protein signals, and then the protein signal on cell 1 was subtracted from the protein signal on cell 2 to obtain the specific signal of interaction. The kinetic data were cleaned up as above and then the kinetic parameters were calculated by a procedure of global fitting, as implemented in the Bia-evaluation 3.0 software (Biacore). For the wild-type Off7(wt) and its cysteine mutants, we applied a simple kinetic model of Langmuir binding to analyze the data. For the preparations of conjugates, we applied a model with two populations of analytes, whose respective proportions were deduced from the coupling yield y_c of the fluorophore and therefore determined independently.

Results

Design of the conjugates

The design and construction of RF biosensors from the DARPin Off7 involved three steps: the choice of a target

Table I. Analysis of the interface between Off7 and MalE in the crystal structure of their complex

Residue	ΔASA (Å^2)	Contact	Set
Arg23	9.1	None	S3
Asn45	9.0	None	S3
Thr46	23.9	HOH15	S2
Thr48	18.6	MalE	S1
Leu53	12.2	None	S3
Tyr56	49.8	MalE	S1
Asp77	9.2	HOH94	S2
Val78	34.2	MalE	S1
Phe79	116.6	MalE	S1
Tyr81	47.0	MalE	S1
Leu86	26.6	MalE	S1
Tyr89	58.7	MalE	S1
Trp90	97.0	MalE	S1
Asp110	10.1	MalE	S1
Ser111	0.8	None	S3
Asp112	17.9	None	S3
Met114	0.7	HOH192	S2
Leu119	0.2	None	S3
Lys122	1.6	HOH29, 132	S2
Trp123	64.3	MalE	S1
Tyr125	13.6	MalE	S1

Column 1, residues of Off7 for which ΔASA ≠ 0. Column 2, variation of ASA between the free and MalE-bound states of Off7 for the residue in column 1. Column 3, molecules in contact with the residue of column 1. Column 4, sub-sets of the residues in column 1: S1, residues in direct contact with MalE; S2, residues in contact with MalE through a water molecule; S3, residues not in contact. The water molecules are numbered according to the PDB file 1SVX. HOH29 and HOH132 belong to a network of six water molecules (HOH20, 110, 29, 132, 147 and 171) that are hydrogen-bonded and located in the interface between Off7 and MalE.

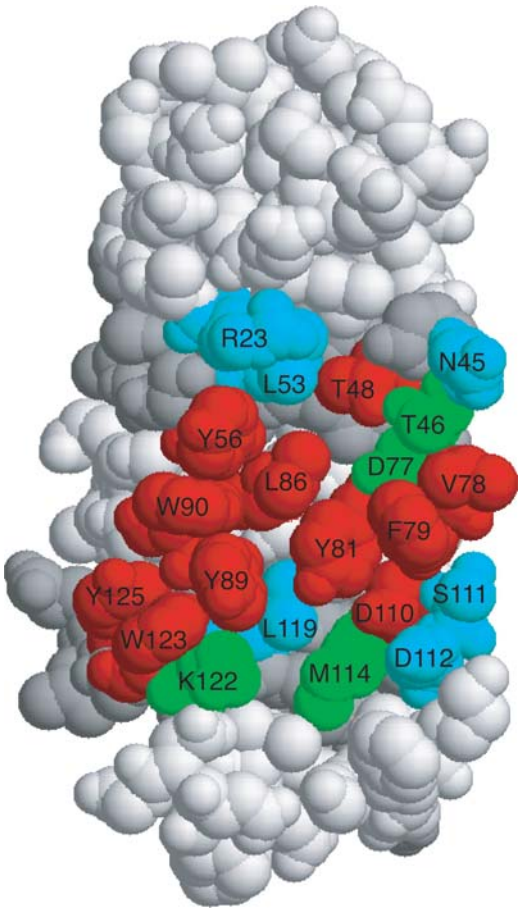

Fig. 1. Positions of the coupling sites in the structure of DapOff7. The ankyrin repeats are represented in alternating light grey and dark grey, with the N-cap on top. Red, residues in direct contact with MalE (subset S1); green, residues in indirect contact with MalE, through a water molecule (S2); blue, residues whose solvent ASA varies on the binding of MalE and which are in contact with MalE neither directly nor indirectly (S3). The residues of S2 and S3 were targeted for the coupling of IANBD. Off7 is seen from the position of MalE in their complex.

residue, the change of this residue into cysteine by site-directed mutagenesis and the chemical coupling of a fluorophore to the mutant Cys. As a first step, we searched for sites in Off7 that satisfied two principles, for the coupling of fluorophores. First, the environment of the coupling residue should change between the free and bound states of Off7, so that the environment of the fluorophore would also change between the free and bound states of the conjugate, after coupling. Second, the coupling residue should not be involved in the interaction between Off7 and MalE, so that the fluorophore would not interfere with the interaction between the conjugate and MalE. We applied these two principles to the crystal structure of the complex between Off7 and MalE. We identified the residues of Off7 whose solvent ASA varied between its free and its MalE-bound states. We divided this initial set *S* of residues into three subsets. Subset S1 contained the residues of *S* in direct contact with MalE. Subset S2 contained the residues of *S* that were in indirect contact with MalE, through a water molecule. Subset S3 contained the residues of *S* without any contact, either direct of indirect, with MalE (Table I, Fig. 1). The classifications of the residues were identical when we considered the whole residues or only their side chains. We targeted the coupling of the fluorophore to the residues of subsets S2 and S3, and rejected those of subsets S1 to avoid affecting the affinity between Off7 and MalE. However, we also rejected one residue of S2 and one of S3 for the following reasons. Asp77 of Off7 was rejected because it is indirectly hydrogen-bonded to Lys202 of MalE through a water molecule (HOH94), and such an indirect hydrogen bond can be energetically important (England *et al.*, 1997). Leu119 was rejected because its ΔASA on MalE binding is very small, 0.2 Å^2. We thus selected eight residues in Off7 as potential coupling sites. As a negative control for our design, we chose residue Lys68, which is located diametrically opposite to the MalE binding site on Off7.

Production and oligomeric state of the cysteine mutants

The eight targeted residues of Off7 and the control residue were changed individually into cysteine by site-directed mutagenesis of the coding gene. The mutant DARPins were produced in the cytoplasm of *E.coli* at 37°C and purified through their hexahistidine tag. The yield of purified soluble protein varied between 30 and 100 mg l^{-1} of culture. It varied as much between different mutants as between different batches of the same mutant, and was consistent with that reported previously for the wild-type Off7(wt) (Binz *et al.*, 2004).

The introduction of a cysteine residue could lead to intermolecular disulfide bonds. To characterize the oligomeric state of the Off7 mutants, we analyzed their purified preparations by SDS–PAGE after denaturation in the presence or absence of a reducing agent. Under reducing conditions, we

Table II. Properties of the cysteine mutants of Off7

Mutation	ASA(S_γ) (Å^2)	Dimer (%)	y_c	y_s
R23C	17.3	69	0.98	0.60
N45C	26.8	63	0.57	0.73
T46C	13.4	25	0.47	0.67
L53C	3.9	8	0.99	0.67
K68C	28.0	11	1.02	0.67
S111C	16.0	6	0.92	0.61
D112C	19.0	7	0.76	0.67
M114C	8.0	4	0.93	0.56
K122C	5.2	3	1.10	0.59

Column 1, mutation in Off7. Column 2, ASA of the S_γ atom, as measured on a three-dimensional model of the Off7 mutant (Materials and methods). Column 3, proportion of polypeptides in a dimeric state, in a purified preparation of the Off7 mutant. Column 4, number of molecules of fluorophore per molecule of Off7 in a purified preparation of the conjugate (coupling yield y_c). Column 5, proportion of protein molecules that remained at the end of the coupling procedure (yield of synthesis y_s).

observed a single protein species with an apparent molecular mass that was consistent with the theoretical mass of an Off7(wt) monomer, 18 272.4. Under non-reducing conditions, we observed a second species with an apparent molecular mass that was consistent with the theoretical mass of a dimer, 36 542.9. The proportion of protomers in a dimeric state was calculated from the intensities of the protein bands. It varied widely between different mutants, from 3% to 64% (Table II).

We modeled the three-dimensional structure of the mutant Off7 molecules and calculated the solvent ASA of the mutant cysteines. A low accessibility of the S_γ atom to the solvent prevented the formation of a dimer whereas a high accessibility was not sufficient to form one (e.g. at positions Lys68, Ser111 and Asp112; Table II). Probably, the geometrical relationships that are necessary to form a disulfide bond were not satisfied for these three last mutations (Sowdhamini *et al.*, 1989).

Conjugation and its yield

We submitted the purified preparations of the Off7 mutants to a reaction of reduction before coupling with the thiol reactive fluorophore IANBD ester, to break open the potential intermolecular disulfide bonds and ensure that the mutant cysteine would be in a reactive state. The products of the coupling reaction were separated from the unreacted fluorophore by chromatography on a nickel ion column. The coupling yield y_c, defined as the number of fluorophore groups per Off7 molecule, was calculated from the absorbance spectrum of the purified reaction product (Materials and methods; Table II). It was very reproducible, close to 100% for six of the nine Off7 mutants, and lower for the mutants at positions Asp112 (75%), Asn45 (57%) and Thr46 (47%). The synthesis yield y_s of the coupling procedure, i.e. the proportion of protein molecules that remained at the end of the procedure, was similar for all the Off7 mutants, $64 \pm 5\%$ [mean $\pm$ standard error (SE), Table II].

We analyzed the cause for the low yield of coupling that we observed in position Asn45 at a 5:1 molar excess of IANBD over Off7. The low yield of coupling for Off7(N45C) did not result from a low accessibility of the mutant cysteine to the solvent, since this mutant derivative of Off7 could form an intermolecular disulfide bond efficiently. It did not result from an irreversible modification of the mutant cysteine since an analysis of a purified preparation of Off7(N45C) by mass spectrometry showed that it contained only two protein species, with molecular masses that were equal to $18\,275.8 \pm 1.6$ and $36\,548.7 \pm 2.1$ and therefore close to the theoretical masses of the monomeric and dimeric states of Off7(N45C), 18 272.4 and 36 542.9, respectively. The low yield did not result from an oxidized state of the mutant cysteine because we performed a reducing treatment either before or during the coupling reaction, with different reducing agents (TCEP or DTT) and at different concentrations of these agents (from 0.1 to 5 mM), without any change. Moreover, we checked by SDS–PAGE that the protein was in a monomeric state immediately after this treatment. Finally, the low yield did not result from slow coupling kinetics because it was not changed by an increase in temperature (from 30°C to 40°C) or the duration of the reaction (from 30 min to overnight). Therefore, we are unable to explain the differences in the yields of coupling at present.

Fluorescence properties of the conjugates

The fluorescence of the conjugates was excited at 485 nm and recorded at 535 nm. We first measured the fluorescence intensity F_0 of the Off7 conjugates in their free state. We then tested the responsiveness of the conjugates to the binding of their MalE antigen by measuring the relative variation $\Delta F/F_0 = (F - F_0)/F_0$ in their fluorescence intensity F between their MalE-bound and free states. In a preliminary test, we used a concentration of MalE equal to 2.6 μM, i.e. about 9 times the concentration of conjugate (0.3 μM) and 230 times the value of the dissociation constant K_d (11 nM) between Off7(wt) and MalE. All the conjugates that we constructed responded to the binding of MalE, except the Off7(K68ANBD) control. The value of $\Delta F_{2.6\mu M}/F_0$ was between 0.9 and 14.6 for the eight responsive conjugates when the assay was done in the low salt buffer L1 (Table III).

The values of $\Delta F_{2.6\mu M}/F_0$ varied between conjugates. These variations could come either from different interactions between the fluorescent group and MalE or from different affinities between the conjugates and MalE. To distinguish between these mechanisms and characterize the properties of the eight conjugates in more detail, we performed titration experiments in buffer L1 (Fig. 2). Equation (7), linking $\Delta F/F_0$ and the concentration of target antigen, was fitted to the experimental data to determine $\Delta F_\infty/F_0$ and K_d (Table III). For seven of the eight conjugates, the values of $\Delta F_\infty/F_0$ and $\Delta F_{2.6\mu M}/F_0$ were close and the K_d values were between 10 and 546 nM, i.e. well below 2.6 μM. These values were consistent with a saturation of the conjugates with MalE at 2.6 μM. Nonetheless, the values of K_d differed significantly between conjugates, with three values being close to the value for the parental Off7(wt) (Table III). Note that the K_d values for the tight binding conjugates could not be accurately determined in this way since the concentration of conjugate was much higher than K_d (see below). In contrast, K_d was equal to 4.7 mM and therefore 1800-fold higher than 2.6 μM for Off7(K122ANBD). Therefore, this conjugate was not saturated by MalE at 2.6 μM, which explained the large difference between its values of $\Delta F_\infty/F_0$ and $\Delta F_{2.6\mu M}/F_0$ (2.2 and 121, respectively). The high value of

Table III. Properties of Off7 conjugates, as derived from fluorescence experiments

Residue	Buffer	f_b (FU μM^{-1})	$\Delta F_{2.6\mu M}/F_0$	$\Delta F_\infty/F_0$	K_d (nM)
Arg23	L1	341 ± 2	0.96 ± 0.03	0.96 ± 0.01	26 ± 4
Asn45	L1	232 ± 6	14.1 ± 0.4	14.00 ± 0.07	13 ± 2
Thr46	L1	166 ± 2	14.5 ± 0.2	18.0 ± 0.2	546 ± 40
Leu53	L1	276 ± 2	2.61 ± 0.05	2.91 ± 0.06	271 ± 36
Ser111	L1	271 ± 1	0.74 ± 0.01	0.73 ± 0.01	10 ± 3
Asp112	L1	197 ± 2	2.09 ± 0.03	2.17 ± 0.04	121 ± 19
Met114	L1	56 ± 5	8.1 ± 0.9	8.9 ± 0.2	211 ± 30
Lys122	L1	47 ± 1	2.21 ± 0.04	122 ± 13	(4.7 ± 0.3) × 10^6
Arg23	M1	314 ± 2	ND	0.93 ± 0.01	18 ± 5
Asn45	M1	266 ± 3	ND	8.25 ± 0.06	8 ± 2
Thr46	M1	323 ± 4	ND	7.92 ± 0.08	255 ± 18
Leu53	M1	259 ± 3	ND	2.61 ± 0.03	104 ± 10
Asn45	Serum	452 ± 4	ND	2.11 ± 0.01	18 ± 2

Column 1, residue with which the fluorophore was coupled. Column 3, molar fluorescence f_b of the free conjugate. The total concentration of conjugate was equal to $0.3y_c$ μM, where the coupling yield y_c is given in Table II. The entries for f_b and $\Delta F_{2.6\mu M}/F_0$ give the mean value and associated SE in at least two experiments. The entries for $\Delta F_\infty/F_0$ and K_d give the value and associated SE from the fitting of Equation (7) to the data points in the titration experiments. The Pearson parameter in these fittings was $R > 0.996$. The K_d value for Off7(wt) was equal to 11 ± 1 nM in buffer L2 and 5.6 ± 0.8 nM in buffer M2, as measured by competition Biacore. Serum, 90% fetal calf serum; ND, not determined. The SE value on $\Delta F_{2.6\mu M}/F_0$ was calculated from the equation of error propagation $[SE(\Delta F_{2.6\mu M}/F_0)]^2 = (F_{2.6\mu M}/F_0)^2\{[SE(F_{2.6\mu M})/F_{2.6\mu M}]^2 + [SE(F_0)/F_0]^2\}$.

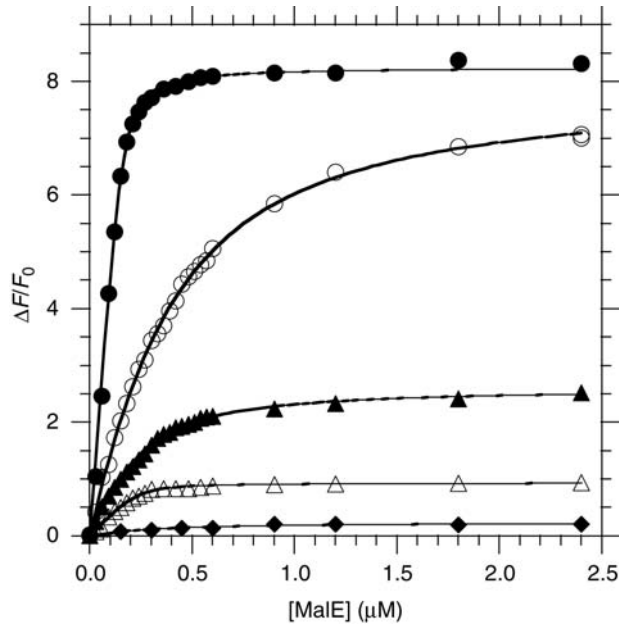

Fig. 2. Titration of Off7 conjugates by MalE, monitored by fluorescence. The experiments were performed at 25°C in buffer M1. The total concentration of Off7, measured by A_{280}, was equal to 0.3 μM. The total concentration in the MalE protein is given along the *x*-axis. The continuous curves correspond to the fitting of Equation (7) to the experimental values of $\Delta F/F_0$ (see Materials and methods for details). Open triangles, position Arg23; closed circles, Asn45; open circles, Thr46; closed triangles, Leu53; closed diamonds, Lys68 (negative control on the backside of the molecule).

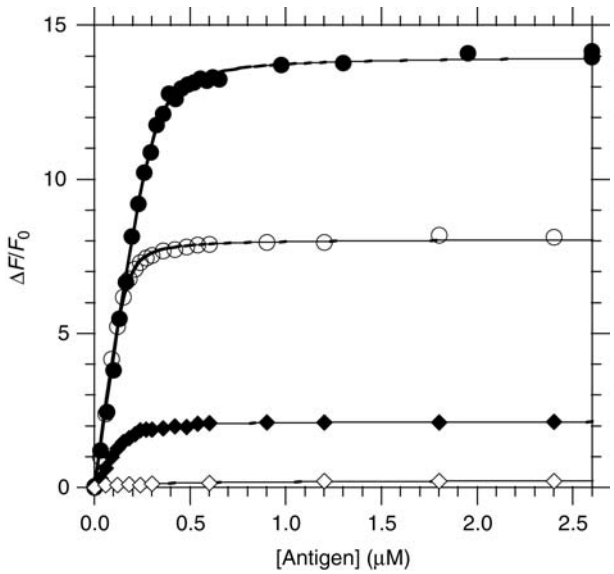

Fig. 3. Selectivity and specificity of the fluorescence signal for the Off7(N45ANBD) conjugate. The experimental conditions were as described in Fig. 2, except for the buffers. The total concentration in antigen, MalE or BSA is given along the *x*-axis. Closed circles, MalE in buffer L1; open circles, MalE in buffer M1; closed diamonds, MalE in 90% serum; open diamonds, BSA in buffer M1.

$\Delta F_\infty/F_0$ for Off7(K122ANBD) was obtained through a long-range extrapolation and might be a large overestimate.

Fluorescence and salt effects

The quantum yield of fluorophores and the electrostatic interactions between molecules can be salt sensitive. The salt concentration of the buffer could therefore affect the response of the Off7 conjugates at the levels of both their fluorescent group and interaction with MalE. To test these assumptions, we compared the fluorescence properties of four conjugates, at positions Arg23, Asn45, Thr46 and Leu53, by titration in low salt buffer L1 and medium salt buffer M1 (Fig. 3). We also compared the properties of interaction between the parental Off7(wt) and MalE in these two buffers by competition Biacore (Materials and methods).

We found that the value of K_d for Off7(wt) was slightly higher in buffer L1 than in buffer M1, 11 ± 1 versus 5.6 ± 0.8 nM, as measured by competition Biacore. We observed the same trend for the K_ds of the four conjugates as measured by titration experiments, e.g. the value of K_d for Off7(T46ANBD) was higher by 2-fold in buffer L1 (Table III). These results suggested that the NaCl ions

screened unfavorable electrostatic interactions. The values of F_0 and $\Delta F_\infty/F_0$ were very close in buffers L1 and M1 for the conjugates at positions Arg23 and Leu53. In contrast, the values of F_0 were lower in buffer L1 than in buffer M1 for the conjugates at positions Asn45 and Thr46, and these lower values of F_0 contributed to the higher values of $\Delta F_\infty/F_0$ in buffer L1, up to 2-fold (Table III). Thus, lower salt concentrations could increase both K_d and $\Delta F_\infty/F_0$ for some conjugates. Possible reasons for the variation of the F_0 value between different conjugates will be considered in the Discussion section.

Selectivity and specificity

The selectivity of a biosensor refers to the extent to which it can recognize a particular analyte in a complex mixture without interference from other components (Vessman *et al.*, 2001). We tried to characterize the selectivity of the Off7(N45ANBD) conjugate by comparing titration with the MalE antigen in serum and in medium salt buffer M1 (Fig. 3). We found that the value of $\Delta F_\infty/F_0$ for Off7(N45ANBD) remained high in serum, 2.11 ± 0.01, and that this conjugate recognized MalE with similar values of K_d in serum and buffer M1 (Table III). Thus, Off7(N45ANBD) recognized MalE selectively in serum. However, the value of F_0, the fluorescence intensity of the free conjugate, was 1.7-fold higher and the value of $\Delta F_\infty/F_0$ was 3.9-fold lower in serum than in buffer M1. Thus, some components of the serum interfered with the fluorescence properties of Off7(N45ANBD) (see below).

To test the specificity of the recognition between the Off7 conjugates and MalE, we titrated Off7(R23ANBD) and Off7(N45ANBD) with BSA and hen egg white lysozyme in buffer M1. We found that the values of $\Delta F_{2.6\mu M}/F_0$ were much lower for the non-cognate proteins than for MalE, e.g. 40-fold lower for BSA (Fig. 3). Therefore, the variation of the $\Delta F/F_0$ signal was indeed specific for MalE, the cognate antigen.

Binding parameters

The experimental conditions of the fluorescence titrations were not optimal to evaluate low nanomolar values of K_d precisely since the concentration of conjugate was micromolar and thus far above K_d. We therefore measured the kinetic parameters of interaction between Off7(wt), four of its cysteine mutants, and the four corresponding conjugates on the one hand, and MalE on the other hand by Biacore in appropriate conditions of concentration to better understand the mechanisms of variation in these parameters (Materials and methods). The kinetics were measured in the presence of DTT for the cysteine mutants to prevent their dimerization. For Off7(wt) and its cysteine mutants, we analyzed the kinetic data with a 1:1 model and calculated the corresponding dissociation constant from the rate constants, i.e. $K_d' = k_{off}/k_{on}$. For the conjugates, we used a model with one ligand (MalE) and two analytes (the Cys mutant of Off7 with or without fluorophore), whose molar ratio was deduced from the coupling yield y_c, to take the incomplete coupling of the preparations into account (Table IV).

We found that the value of K_d, measured at equilibrium in solution by competition Biacore (legend to Table III), and the value of K_d', deduced from kinetic experiments at the interface between a liquid and a solid phase (Table IV), were close for Off7(wt) in medium salt buffer (5.6 ± 0.8 versus 7.7 nM) and consistent with values reported previously (Binz *et al.*, 2004). The value of K_d' for Off7(wt) was higher in low salt buffer than in medium salt buffer. This variation of K_d' with the concentration in salt was consistent with that of K_d, determined by competition Biacore, although larger (3.5-fold versus 2-fold; legend to Tables III and Table IV). It was mainly due to an increase in k_{on} with the concentration in salt and therefore consistent with a long range effect, e.g. the screening of unfavorable electrostatic interactions between Off7(wt) and MalE by the salt. The other kinetics were measured only in medium salt buffer. The mutations into Cys had little effect on the values of k_{off}, k_{on} and K_d'. The effects on K_d' were the most important for mutations N45C and T46C (2.2-fold) and mainly due to a slower k_{on}.

For the preparations of conjugates, the value of K_{d1}', measured by Biacore and corresponding to the fraction of conjugated molecules, was consistent with that of K_d, measured by fluorescence. The value of K_{d2}', corresponding to the non-conjugated molecules, was close to that of K_d' for the parental cysteine mutant, except for the preparation of Off7(T46ANBD) for which it was 4-fold higher. Because these kinetic experiments were performed in the absence of a reducing agent, the non-coupled molecules of Off7(T46ANBD) could be in a dimeric state and thus be altered in their ability to bind MalE. The value of K_{d1}' for Off7(N45ANBD) was close to that of K_d' for Off7(wt); it was 8-fold higher for Off7(R23ANBD) and about 50-fold higher for Off7(T46ANBD) and Off7(L53ANBD). The increase in the K_{d1}' value of the conjugates relative to the K_d' value of the parental Off7(wt) resulted from variations in both k_{off1} and k_{on1}, and the variation of this latter parameter was important, 10-fold, when comparing Off7(T46ANBD) and Off7(wt).

A comparison between the values of K_d' for the cysteine mutants and K_d or K_{d1}' for the conjugates showed that the variations in affinity relative to Off7(wt) were mainly due to the coupling of the fluorophore and not to the mutation into Cys. The values of K_d, determined by fluorescence titration experiments, were in-between the corresponding values of K_{d1}' and K_{d2}', determined by Biacore. This comparison was consistent with K_d being an apparent dissociation constant and describing a mixture of conjugated and unconjugated molecules, where the latter acted as a competitor of the former. However, one should keep in mind that dissociation constants in solution and at the interface between solid and liquid phases are not generally equal (Rich and Myszka, 2005).

Mechanism of fluorescence variation

All eight conjugates that we designed as potential biosensors were sensitive to the binding of MalE, with $\Delta F_\infty/F_0$ between 0.73 and 14. To test whether these variations of fluorescence resulted from the proximity between the coupling site of the fluorophore and the binding site of MalE, as assumed in our design, we constructed the Off7(K68ANBD) conjugate as a control. Residue Lys68 is located diametrically opposite to the binding site of MalE on Off7. We did not observe any variation of fluorescence for Off7(K68ANBD) with the binding of MalE. This observation showed that the fluorophore had to be in the neighborhood of the DARPin binding site for the fluorescence to vary.

Table IV. Binding parameters of Off7 and derivatives, as determined by Biacore experiments

Derivative	Buffer	Model	k_{on1} (10^5 M^{-1} s^{-1})	k_{off1} (10^{-3} s^{-1})	K_{d1}' (nM)	k_{on2} (10^5 M^{-1} s^{-1})	k_{off2} (10^{-3} s^{-1})	K_{d2}' (nM)
WT	M2	LB	6.6	5.1	7.7	NA	NA	NA
WT	L2	LB	2.5	6.2	25.1	NA	NA	NA
WT	M3	LB	5.5	6.1	11.1	NA	NA	NA
R23C	M3	LB	4.1	5.0	12.4	NA	NA	NA
N45C	M3	LB	2.9	7.4	25.7	NA	NA	NA
T46C	M3	LB	1.7	4.1	24.7	NA	NA	NA
L53C	M3	LB	3.7	6.9	18.8	NA	NA	NA
R23ANBD	M2	HA	1.8	11.7	63.2	4.3	2.7	6.2
N45ANBD	M2	HA	2.1	1.8	8.9	2.4	11.3	46
T46ANBD	M2	HA	0.64	26.1	408	0.18	1.8	98
L53ANBD	M2	HA	2.0	60	326	5.8	4.0	6.8

bt-MalE was immobilized on streptavidin SA sensorchips. The association and dissociation rate constants, k_{on} and k_{off}, were determined at 25°C and used to calculate $K_d' = k_{off}/k_{on}$ (Materials and methods). We applied a simple kinetic model of Langmuir binding (LB) for Off7(wt) and its cysteine mutants. This simple model led to single rate constants of association and dissociation, k_{on1} and k_{off1}, respectively. We applied a model with two populations of analytes (heterogeneous analyte HA) for the preparations of conjugates to take incomplete coupling into account. This more complex model resulted in two couples of rate constants: k_{on1} and k_{off1} corresponded to the more abundant species, i.e. the conjugated molecules, whereas k_{on2} and k_{off2} corresponded to the less abundant species, i.e. the unconjugated molecules. For Off7(N45ANBD) and Off7(T46ANBD), the assignment of the rate constants to a particular molecular species was done by comparison with the results obtained for the Cys mutants in the Biacore experiments (this table) and those obtained for the conjugates in the fluorescence experiments (Table III). NA, not applicable.

We used KI to explore the physico-chemical mechanism by which the fluorescence intensity of the conjugates varied on antigen binding. First, we checked by an indirect ELISA that KI, up to 250 mM, did not affect the interaction between the parental Off7(wt) and MalE (Materials and methods). We found that the fluorescence of the Off7(N45ANBD) conjugate was quenched by KI, both in its free and MalE-bound states. The quenching varied linearly with the concentration of KI (Fig. 4). This law of variation indicated that the molecules of fluorophore were identically exposed to KI and constituted a homogeneous population in either case (Lakowicz, 1999). It confirmed that the fluorescent group was specifically coupled to the mutant cysteine. The Stern–Volmer constant was higher for the free conjugate than for its complex with the target antigen: $K_{SV} = 2.92 \pm 0.06$ versus $1.06 \pm 0.03\ M^{-1}$ (SE in the curve fits of Fig. 4). These values indicated a lower accessibility of the fluorophore to KI in the bound state of the conjugate than in its free state. They showed that the fluorescence increase was due to a shielding of the fluorescent group from the solvent by the binding of the antigen, as previously observed for other conjugates with IANBD (Renard *et al.*, 2003). Thus, the mechanism of fluorescence variation was consistent with our rules of design.

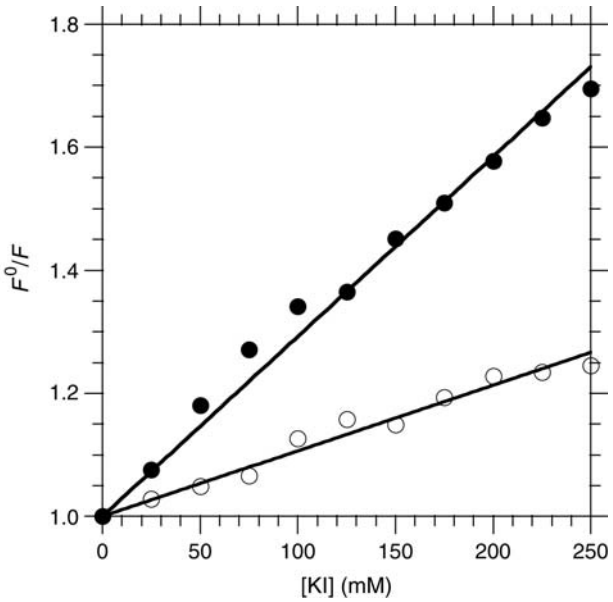

Fig. 4. Quenching of the Off7(N45ANBD) fluorescence by KI. F and F^0, fluorescence of the conjugate at 25°C in buffer M1, with and without quencher, respectively. Closed circles, conjugate (1 μM) in the absence of the MalE antigen; open circles, conjugate (0.3 μM) in the presence of a saturating concentration of MalE (1.8 μM). The continuous curves were obtained by fitting Equation (13) to the experimental data.

Mechanism of fluorescence variation in serum

The profiles of titration of Off7(N45ANBD) by MalE were different in calf serum and in a defined buffer (Fig. 3). In particular, we observed that the value of F_∞ was lower and that of F_0 higher in serum. To better understand these differences, we measured the variations of the F_0 and $F_{2.6\mu M}$ parameters as functions of the concentration in serum (Fig. 5). We observed that the value of $F_{2.6\mu M}$ for Off7(N45ANBD) decreased linearly with the concentration in serum. As expected, the absorbance of the serum alone increased linearly with its concentration, in agreement with the Beer–Lambert law, at both 485 and 535 nm, which were the wavelengths of fluorescence excitation and emission in our experiments. Therefore, the absorption of the excitation and emission lights by serum could account for the variation of $F_{2.6\mu M}$. Surprisingly, F_0 increased with the concentration in serum, up to 40% (v/v) of serum, and then decreased slightly. The increase could result from the interaction between the fluorescent group and molecules of the serum, and the decrease from the absorbance of the serum, as observed for $F_{2.6\mu M}$.

Discussion

Rules of design and their efficiency

We have developed and validated a method to choose coupling sites for fluorophores in a DARPin and transform it into

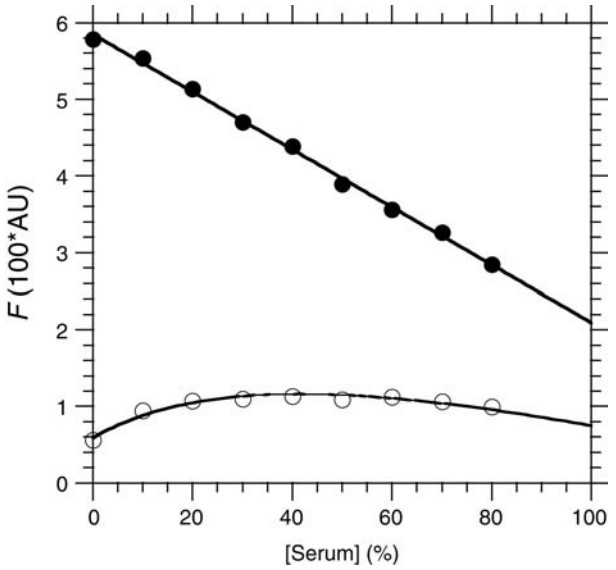

Fig. 5. Effect of the concentration in serum on the fluorescence signals for the Off7(N45ANBD) conjugate. The experiments were performed in a mixture (v:1 − v) of serum and buffer M1. The total concentration of MalE was equal to 2.6 μM and thus saturating. The other experimental conditions were as described in Fig. 2. Open circles, F_0; closed circles, $F_{2.6\mu M}$; AU, arbitrary units of fluorescence. The continuous curves were drawn only for clarity.

an RF biosensor. The method is based on the crystallographic coordinates of the complex between the DARPin and its target antigen, and it does not involve any knowledge on the energetic contributions of residues in the interface. Two criteria were applied: (i) the solvent ASA of the target residue should vary between the free and bound states of the DARPin; and (ii) the target residue should not be in direct contact with the antigen. The first rule was based on the assumption that the fluorescence variation of the conjugate upon antigen binding is due to a change in the environment of the fluorescent group. The second one aimed at avoiding residues that contribute to the energy of interaction between the DARPin and its antigen.

We applied this method to the complex between Off7 and MalE, and thus selected eight coupling residues in Off7. Each of them resulted in a conjugate that could detect the binding of MalE with a value $\Delta F_\infty/F_0 > 0.73$, and most of them much higher. Three conjugates had affinities close to that of Off7(wt) ($\Delta\Delta G \leq 0.5$ kcal mol^{-1}). The most promising conjugate, Off7(N45ANBD), had a value $\Delta F_\infty/F_0 = 14.0 \pm 0.1$ and an affinity nearly identical to that of Off7(wt). Experiments of fluorescence quenching by KI with the Off7(N45ANBD) conjugate showed that the mechanism of fluorescence variation was consistent with our rules of design.

We constructed three conjugates from residues that were indirectly in contact with the antigen, through a bridging water molecule (Thr46, Met114 and Lys122, belonging to subset S2). Remarkably, these three conjugates had the highest values of $\Delta F_\infty/F_0$ and the lowest values of F_0 (listed as the molar quantity f_b in Table III). Residues Thr46 and Met114 make indirect contacts with MalE through a single and isolated water molecule (HOH15 and HOH192, respectively). Lys122 makes indirect contacts with MalE through two water molecules (HOH29 and HOH132) which in turn belong to a network of six water molecules, linked by hydrogen bonds. The corresponding conjugate Off7(K122ANBD) had an exceptionally high value of $\Delta F_\infty/F_0$ (obtained through a long-range extrapolation, see Results). The low F_0 values suggested that the fluorescent group was highly exposed to the solvent in the free state of these conjugates. The positions of the water molecules and high $\Delta F_\infty/F_0$ values suggested that the fluorescent group displaced water molecules in the interface between Off7 and MalE in the bound state of these conjugates, and was at least partially buried in this interface. Consistent with this hypothesis, the affinities between the three corresponding conjugates and MalE were also much decreased relative to Off7(wt).

Residue Asn45 is adjacent to residue Thr46 but farther from the interface between Off7 and MalE than the latter. The corresponding conjugate Off7(N45ANBD) had a very high value $\Delta F_\infty/F_0 = 14.0 \pm 0.1$ and an unchanged affinity relative to Off7(wt). Its fluorescent group might have replaced HOH15 in the interface between Off7 and MalE, as described above for Off7(T46ANBD), but without hindering their interaction. The high values of $\Delta F_\infty/F_0$ that we obtained for some conjugates showed that the use of the IANBD ester as a fluorophore did not limit the extent of the fluorescence response *a priori*.

Impact of the fluorescent group on antigen binding

The $\Delta F_\infty/F_0$ and K_d parameters were obtained by fitting Equation (7) to titration data. This equation assumes homogeneous preparations of conjugate, whereas they contained both the conjugated species and the cysteine mutant in an unconjugated state when the coupling yield was lower than 1. The value of $\Delta F_\infty/F_0$, which is a relative dimensionless parameter, was not affected by the coupling yield. The concentration of antigen that was available to the conjugate was lower than or equal to the total concentration because of the competition with the unconjugated cysteine mutant. Therefore, the real value of K_d for the interaction between a conjugate and MalE was necessarily lower than the apparent value of K_d that we obtained with Equation (7). Hence, the values of $\Delta F_\infty/F_0$ that we report are correct values, despite our approximation of homogeneous preparations while the values of K_d are upper limits, i.e. the real affinities of the conjugates for MalE were higher than or equal to the apparent affinities that we report (Table III). The values of K_d for the Off7 conjugates in the titration experiments were compatible with their K_{d1}' values in the Biacore experiments. Moreover, the K_{d2}' values for the conjugates were consistent with the K_d' values for the unconjugated cysteine mutants in the Biacore experiments (Tables III and IV). These comparisons indicated that the parameters that we determined to characterize the conjugates were reliable.

We found that the K_d' values, measured for four of the cysteine mutants, were only 1.1- to 2.3-fold higher than the K_d' value for Off7(wt). Therefore, the differences between the K_{d1}' values for the conjugates at positions 23, 46 and 53 and the K_d' value for Off7(wt) were mainly due to the presence of the fluorescent group, which affected the interaction between Off7 and MalE.

Classification of the conjugates

The conjugates of Off7 gave a wide range of values for $\Delta F_\infty/F_0$ and K_d. We classified them according to their

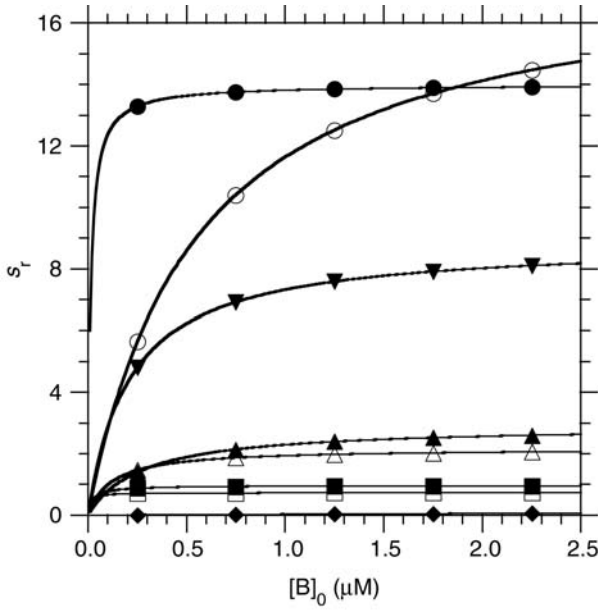

Fig. 6. Relative sensitivities s_r of the Off7 conjugates at 25°C in buffer L1 as a function of their concentration. This figure is a plot of Equation (10), using the parameters listed in Table III. The s_r parameter relates the relative variation of fluorescence intensity $\Delta F/F_0$ and the relative concentration of antigen $[A]_0/[B]_0$ for the low values of $[A]_0$, where $[A]_0$ and $[B]_0$ are the total concentration of antigen and conjugate in the binding reaction, respectively [Equations (9) and (10)]. Closed squares, position Arg23; closed circles, Asn45; open circles, Thr46; closed triangles, Leu53; open squares, Ser111; open triangles, Asp112; closed inverted triangles, Met114; closed diamonds, Lys122.

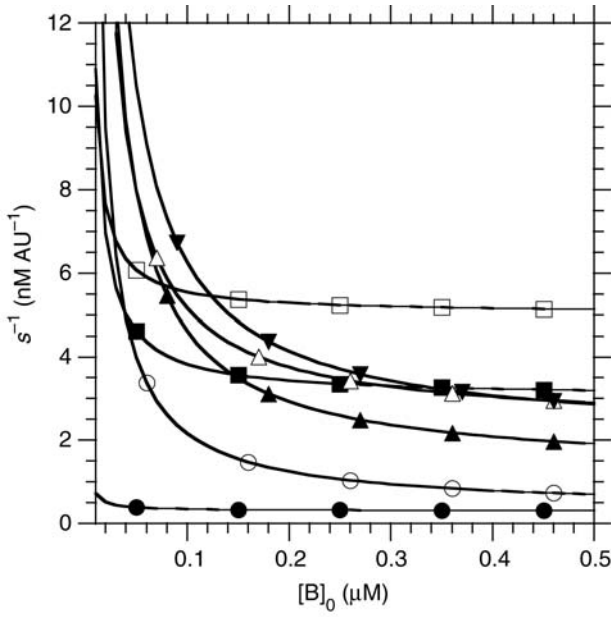

Fig. 7. Comparison of the lower limits of detection for the Off7 conjugates at 25°C in buffer L1 as a function of their concentration. This figure is a plot of Equation (11), using the parameters listed in Table III. The s^{-1} parameter gives the lowest concentration of antigen $[A]_0$ that can be detected by a conjugate when the lowest variation of fluorescence intensity that can be detected by the spectrofluorometer is equal to 1 FU [Equations (11) and (12)]. Closed squares, position Arg23; closed circles, Asn45; open circles, Thr46; closed triangles, Leu53; open squares, Ser111; open triangles, Asp112; closed inverted triangles, Met114.

sensitivity, a parameter which is used to characterize any measuring instrument. This sensitivity can take two forms for an RF biosensor, a relative sensitivity s_r and an absolute sensitivity s. The relative sensitivity s_r relates the relative variation $\Delta F/F_0$ of the fluorescence signal to the relative concentration $[A]_0/[B]_0$ of antigen for the low values of the latter, where $[A]_0$ and $[B]_0$ are the total concentrations of antigen and conjugate, respectively, in the titration reaction [Equation (9) in Materials and methods; $[A]_0/[B]_0$ can be viewed as the concentration of antigen, normalized to the concentration of conjugate]. s_r is an intrinsic dimensionless parameter. Its value does not depend on the spectrofluorometer or its set-up, and should remain constant between experiments, instruments and laboratories. The value of s_r depends on the values of $[B]_0$ and K_d according to a saturation law and its maximal value is equal to $\Delta F_\infty/F_0$ [Equation (10)]. The absolute sensitivity s relates ΔF and $[A]_0$ for the low values and is equal to $f_b s_r$, where f_b is the molar fluorescence of the free conjugate [Equations (8) and (11)]. The s^{-1} parameter relates the lower limit of detection $\delta[A]_0$ for the conjugate to the lower limit of measurement δF for the spectrofluorometer.

We calculated the variations of s_r and s^{-1} for each conjugate as functions of $[B]_0$ in the low salt buffer L1 from Equations (10) and (11) (Figs 6 and 7). These variations showed that the classification of the conjugates according to their values of s_r and s^{-1} varied as a function of $[B]_0$. For s_r and with $[B]_0 =$ 0.3 μM, i.e. the concentration at which we performed our experiments, the coupling positions ranked in the following decreasing order, i.e. starting with the highest relative sensitivity: Asn45 > Thr46 > Met114 > Leu53 ≈ Asp112 > Arg23 > Ser111. For s^{-1} and $[B]_0 = 0.3$ μM, the coupling positions ranked in the following increasing order, starting with the lowest limit of detection: Asn45 < Thr46 < Leu53 < Arg23 ≈ Asp112 ≈ Met114 < Ser111. The Off7(N45ANBD) conjugate at 0.3 μM had a value $s_r = 13.4$ and therefore a lower limit of detection $\delta[A]_0 = 0.34$ nM since our Perkin-Elmer SF5B spectrofluorometer could detect a relative variation of fluorescence $\delta F/F_0 = 1.5\%$ in our experimental conditions [Equation (12)]. The ranking of the conjugates according to s^{-1} was valid because all our measurements were done with the same spectrofluorometer, set-up of the instrument and rhodamine 101 as an internal standard.

Coupling sites in the absence of structural data

To be useful, the approach that we developed and validated with Off7 should be generalizable to DARPins for which the structure of the complex with the antigen is unknown, because such structural data are not always available. Each ankyrin repeat module, except the N-cap and C-cap modules, comprises 33 residues. The positions that are randomized to construct combinatorial libraries of DARPins correspond to potential residues of interaction with the antigen and they occupy positions 2, 3, 5, 13, 14, 26 and 33 of each module (Binz *et al.*, 2004). Let us consider the set R of these randomized positions. Several residues of Off7 that occupy R positions are in contact with MalE either directly (subset $R \cap S1$) or through a water molecule (subset $R \cap S2$) in the structure of their complex, as expected. Three residues that occupy R positions, Asn45, Ser111 and Asp112, show a variation of their solvent ASA upon binding of the antigen MalE without being in contact with it (subset $R \cap S3$; Table I and

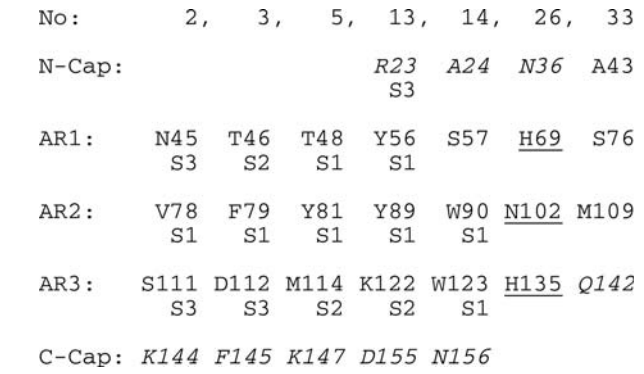

Fig. 8. Comparison between the randomized positions in DARPins and coupling sites in Off7. AR1, AR2 and AR3, ankyrin repeats 1, 2 and 3. Positions 2, 3, 5, 13, 14 and 33 in each ankyrin repeat are fully randomized and represented in roman type. Position 26 is partially randomized and in underlined type. The positions in the N-cap and C-cap that are structurally equivalent to the above positions but not randomized are in italic type. Position 43 in the N-cap module is fully randomized and position 142 in AR3 is not randomized (Binz *et al*., 2004). The figure gives the subset, S1, S2 or S3, to which the corresponding residues of Off7 belonged (see Results and Table I). Residues Asn45, Ser111 and Asp112 are not in contact with MalE (subset S3) and gave acceptable conjugates (see Table III, Figs 6 and 7).

Fig. 8). The conjugates at these three positions had s_r values that were acceptable for biosensors (Table III, Fig. 6). Therefore, our results suggested that it would be possible to obtain RF biosensors from DARPins whose three-dimensional structure is unknown, by targeting in priority the randomized residues that are not important for the interaction with the corresponding antigen, as determined by site-directed mutagenesis.

Conclusions

We have developed a method to construct RF biosensors from DARPins when the crystal structure of the complex with the target antigen is available. This method could be applied to other antigen binding proteins under the same conditions. It could also be extended to DARPins without a known structure of the complex, because of the highly conserved geometry of the binding site. We validated the method by constructing eight conjugates between the IANBD fluorophore and Off7, a DARPin that is directed against the MalE protein from *E.coli*. One of the conjugates showed a relative sensitivity $s_r \geq 6$ when its concentration was $\geq$10 nM, and $s_r \geq 12$ for a concentration $\geq$100 nM. These values of s_r corresponded to lower limits of detection below 0.34 nM in our experimental conditions. The conjugate could function in a complex mixture like serum, albeit at lower relative sensitivity presumably because of an internal absorption of light. The yields of production of Off7 and its cysteine mutants (30–100 mg/L of culture, see Results) and the yields of synthesis of the conjugates with the IANBD fluorophore (64 $\pm$ 2%, mean $\pm$ SE; Table II) were much higher than those for scFv fragments of antibodies (<1.0 mg/l and 24 $\pm$ 2%, respectively) (Renard *et al*., 2003, 2002). Therefore, the DARPins, which are very stable proteins, constitute a promising alternative to antibody fragments for the construction of RF biosensors, directed against any protein antigen. These RF biosensors can be used for the quantification of target molecules in complex mixtures and in real time. They could be used in different formats—in solution, in the form of protein chips or at the tip of optical fibers (Renard *et al*., 2002; Zhu and Snyder, 2003; Vo-Dinh and Kasili, 2005; de Lorimier *et al*., 2006)—with numerous applications in health, environment, industry, defense and fundamental research (Griffiths and Hall, 1993; Morgan *et al*., 1996; Renard *et al*., 2003).

Acknowledgements

We thank Patrick England and Sylviane Hoos for their help with the Biacore instrument; Elodie Monsellier for advice and Nicole Guiso for her constant interest.

Funding

This work was funded by grants from the Délégation Générale à l'Armement, French Ministry of Defense (research contract number DGA-REI 2008.34.0010 to H.B., DGA doctoral fellowship to E.B.-L.), and from Institut Pasteur (DARRI-2007 to H.B.).

References

Altschuh,D., Oncul,S. and Demchenko,A.P. (2006) *J. Mol. Recognit.*, **19**, 459–477.
Binz,H.K., Stumpp,M.T., Forrer,P., Amstutz,P. and Plückthun,A. (2003) *J. Mol. Biol.*, **332**, 489–503.
Binz,H.K., Amstutz,P., Kohl,A., Stumpp,M.T., Briand,C., Forrer,P., Grütter,M.G. and Plückthun,A. (2004) *Nat. Biotechnol.*, **22**, 575–582.
Binz,H.K., Amstutz,P. and Plückthun,A. (2005) *Nat. Biotechnol.*, **23**, 1257–1268.
Bullock,W.O., Fernandez,J.M. and Short,J.M. (1987) *Biotechniques*, **5**, 376–379.
de Lorimier,R.M., *et al*. (2002) *Protein Sci.*, **11**, 2655–2675.
de Lorimier,R.M., Tian,Y. and Hellinga,H.W. (2006) *Protein Sci.*, **15**, 1936–1944.
England,P., Brégégère,F. and Bedouelle,H. (1997) *Biochemistry*, **36**, 164–172.
Foote,J. and Winter,G. (1992) *J. Mol. Biol.*, **224**, 487–499.
Griffiths,D. and Hall,G. (1993) *Trends Biotechnol.*, **11**, 122–130.
Harlow,E. and Lane,D. (1988) *Antibodies: A Laboratory Manual*. Cold Spring Harbor Laboratory, Cold Spring Harbor, NY.
Jespers,L., Bonnert,T.P. and Winter,G. (2004) *Protein Eng. Des. Sel.*, **17**, 709–713.
Kohl,A., Binz,H.K., Forrer,P., Stumpp,M.T., Plückthun,A. and Grütter,M.G. (2003) *Proc. Natl Acad. Sci. USA*, **100**, 1700–1705.
Lakowicz,J.R. (1999) *Principles of Fluorescence Spectroscopy*, 2nd edn. Kluwer Academic/Plenum, New York.
Li,J., Mahajan,A. and Tsai,M.D. (2006) *Biochemistry*, **45**, 15168–15178.
Lisova,O., Hardy,F., Petit,V. and Bedouelle,H. (2007) *J. Gen. Virol.*, **88**, 2387–2397.
Lowe,C.R. (1984) *Trends Biotechnol.*, **2**, 59–65.
Mathonet,P. and Fastrez,J. (2004) *Curr. Opin. Struct. Biol.*, **14**, 505–511.
Morgan,C.L., Newman,D.J. and Price,C.P. (1996) *Clin. Chem.*, **42**, 193–209.
Mosavi,L.K., Minor,D.L. Jr and Peng,Z.Y. (2002) *Proc. Natl Acad. Sci. USA*, **99**, 16029–16034.
Mosavi,L.K., Cammett,T.J., Desrosiers,D.C. and Peng,Z.Y. (2004) *Protein Sci.*, **13**, 1435–1448.
Nieba,L., Krebber,A. and Plückthun,A. (1996) *Anal. Biochem.*, **234**, 155–165.
Pace,C.N., Vajdos,F., Fee,L., Grimsley,G. and Gray,T. (1995) *Protein Sci.*, **4**, 2411–2423.
Renard,M. and Bedouelle,H. (2004) *Biochemistry*, **43**, 15453–15462.
Renard,M., Belkadi,L., Hugo,N., England,P., Altschuh,D. and Bedouelle,H. (2002) *J. Mol. Biol.*, **318**, 429–442.
Renard,M., Belkadi,L. and Bedouelle,H. (2003) *J. Mol. Biol.*, **326**, 167–175.
Rich,R.L. and Myszka,D.G. (2005) *J. Mol. Recognit.*, **18**, 431–478.
Rondard,P. and Bedouelle,H. (1998) *J. Biol. Chem.*, **273**, 34753–34759.
Smith,P.A., Tripp,B.C., DiBlasio-Smith,E.A., Lu,Z., LaVallie,E.R. and McCoy,J.M. (1998) *Nucleic Acids Res.*, **26**, 1414–1420.

Smith,J.J., Conrad,D.W., Cuneo,M.J. and Hellinga,H.W. (2005) *Protein Sci.*, **14**, 64–73.
Sowdhamini,R., Srinivasan,N., Shoichet,B., Santi,D.V., Ramakrishnan,C. and Balaram,P. (1989) *Protein Eng.*, **3**, 95–103.
Steiner,D., Forrer,P. and Plückthun,A. (2008) *J. Mol. Biol.*, **382**, 1211–1227.
Stumpp,M.T., Binz,H.K. and Amstutz,P. (2008) *Drug Discov. Today*, **13**, 695–701.
Thevenot,D.R., Toth,K., Durst,R.A. and Wilson,G.S. (2001) *Biosens. Bioelectron.*, **16**, 121–131.
Vessman,J., Stefan,R.I., Van Staden,J.F., Danzer,K., Lindner,W., Burns,D.T., Fajgelj,A. and Müller,H. (2001) *Pure Appl. Chem.*, **73**, 1381–1386.
Vo-Dinh,T. and Kasili,P. (2005) *Anal. Bioanal. Chem.*, **382**, 918–925.
Vriend,G. (1990) *J. Mol. Graph.*, **8**, 52–56. 29.
Zahnd,C., Amstutz,P. and Plückthun,A. (2007) *Nat. Methods*, **4**, 269–279.
Zhu,H. and Snyder,M. (2003) *Curr. Opin. Chem. Biol.*, **7**, 55–63.